

000 001 002 003 004 005 006 007 008 009 010 011 012 013 014 015 016 017 018 019 020 021 022 023 024 025 026 027 028 029 030 031 032 033 034 035 036 037 038 039 040 041 042 043 044 045 046 047 048 049 050 051 052 053 GAVEL: TOWARDS RULE-BASED SAFETY THROUGH ACTIVATION MONITORING

Anonymous authors

Paper under double-blind review

ABSTRACT

Large language models (LLMs) are increasingly paired with activation-based monitoring to detect and prevent harmful behaviors that may not be apparent at the surface-text level. However, existing activation safety approaches, trained on broad misuse datasets, struggle with poor precision, limited flexibility, and lack of interpretability. This paper introduces a new paradigm: rule-based activation safety, inspired by rule-sharing practices in cybersecurity. We propose modeling activations as cognitive elements (CEs), fine-grained, interpretable factors such as “*making a threat*” and “*payment processing*”, that can be composed to capture nuanced, domain-specific behaviors with higher precision. Building on this representation, we present a practical framework that defines predicate rules over CEs and detects violations in real time. This enables practitioners to configure and update safeguards without retraining models or detectors, while supporting transparency and auditability. Our results show that compositional rule-based activation safety improves precision, supports domain customization, and lays the groundwork for scalable, interpretable, and auditable AI governance. We open source GAVEL and provide an automated rule creation tool.

1 INTRODUCTION

Large language models (LLMs) are often equipped with safeguards that monitor their inputs and outputs to prevent harmful behavior. However, these safeguards can be bypassed through representation attacks, where harmful concepts are paraphrased or obfuscated, exploiting mismatched generalization between surface text and model reasoning. To address this, recent work has shifted towards activation-based monitoring, which detects when the model internally processes restricted concepts (e.g., planning a crime or generating hate speech), regardless of the exact surface form.

The Problem: The prevailing approach to activation safety relies on passing misuse datasets through the model to capture the distribution of activations, which are then modeled with a linear probe or classifier. While influential, this approach suffers from three major limitations:

1. **Poor Precision:** Misuse datasets are typically broad, covering generic categories such as “cybercrime” or “misinformation.” As a result, detectors trained on these distributions often produce many false positives. For example, a detector trained on a hate speech dataset¹ to prevent users from generating racist content will accidentally flag benign discussions about ethnic cultures. To be a viable safeguard, activation-based safety must have low false positive rates.
2. **Limited Flexibility:** In practice, model owners often need to enforce nuanced or domain-specific safety and policy constraints, for instance, detecting intellectual property infringement on specific entities, or enforcing a company’s internal policies. Current methods require *reusing* coarse-grained misuse datasets which do not match the target behavior, or require constructing new, specialized datasets which is a slow and expensive process. Moreover, scaling to many categories is impractical, since thousands of activations must be collected per category to gener-

¹Commonly used hate speech datasets include:

https://huggingface.co/datasets/tdavidson/hate_speech_offensive
<https://huggingface.co/datasets/ucberkeley-dlab/measuring-hate-speech>
https://huggingface.co/datasets/Doowon96/hate_speech_labeled

054 alize well, and retraining detectors is needed for each update. A practical system should instead
 055 allow rapid, configurable deployment that builds on prior work provided by the community.
 056

057 **3. Lack of Interpretability:** When detectors fail, the reasons are often opaque. For example,
 058 a system might flag an input as “hate speech” without indicating which parts of the text are
 059 responsible. The absence of such token-level signals leaves users uncertain about what specif-
 060 ically triggered the alarm. This opacity hinders auditing and accountability, capabilities that
 061 are critical for future agentic systems, where intermediate reasoning steps may be difficult for
 062 humans to interpret (Hao et al., 2024; Chen et al., 2025). Activation safety therefore requires
 063 human-interpretable factors that support customization, transparency, and auditability.

064 **Towards Rule-Based AI Safety:** Our motivation comes from the field of cybersecurity, which has
 065 long benefited from rule sharing for threat detection. Tools such as Snort (Roesch et al., 1999),
 066 YARA (Alvarez & VirusTotal, 2008), and OSSEC (Cid & Team, 2004) allow defenders to share
 067 rule sets which has enabled the community to collaborate on detect threats and perform standardized
 068 security auditing. This ecosystem has proven effective at scaling security across organizations, while
 069 ensuring precision, flexibility, and interpretability.

070 We argue that, in many situations, AI safety can benefit from adopting a similar paradigm. To
 071 improve robustness, the AI community needs the ability to share and collaborate over standardized,
 072 configurable, and model-agnostic rules that define and enforce safety or policy constraints, allowing
 073 interpretability, flexibility and precision. For example, large language models have recently been
 074 used to automate scams (Gressel et al., 2024; Roy et al., 2024). To detect such misuse, a rule might
 075 specify that the model must not consider $(A \text{ OR } (B \text{ AND } C))$, while still permitting C alone
 076 to avoid false positives. This level of expressivity is especially crucial for AI governance, where
 077 regulators and organizations require mechanisms to define and audit policies through transparent
 078 rule sets.

079 **Contributions.** We take the first steps towards the first rule-based safety framework over model
 080 activations, making three primary contributions:

081 **1. Cognitive Elements (CEs):** We introduce the concept of *cognitive elements*, interpretable
 082 activation-level primitives that capture mid-level aspects such as a model’s activity, task, or
 083 behavior. For example, *directing* a user to go somewhere, *acquiring* payment information,
 084 *making* a threat, or *engaging* in coercion. Unlike coarse misuse categories, CEs provide a com-
 085 positional basis: they activate predictably as the model performs, can be combined to describe
 086 complex states, and enable safety systems that are precise, flexible, and interpretable (i.e., if a
 087 rule violation occurs we can see why).

088 **2. Rule-Based Detection Framework:** Building on CEs, we propose **GAVEL**², a framework
 089 that expresses safety and policy constraints as logical rules over CE activations. This enables
 090 practitioners and regulators to (i) configure nuanced constraints without retraining models *or*
 091 detectors, (ii) share standardized rulesets across organizations, and (iii) audit model behavior
 092 through interpretable rule violations. We found that our framework is not only effective, but
 093 can also operate alongside LLMs in real-time.

094 **3. Open Resources for the Community:** To catalyze progress, we release code and tools for
 095 constructing CEs, collecting activations, composing rules, and detecting violations. We further
 096 provide an initial CE vocabulary and prototype misuse rulesets as a foundation for industry and
 097 academic collaboration, inspired by community-driven threat intelligence in cybersecurity.

098 In summary, our central insight is that LLM behaviors can be detected by decomposing them into
 099 independent elemental concepts. This not only improves precision but also decouples activation
 100 engineering (constructing activation datasets) from safety configuration (defining rules). As a result,
 101 GAVEL enhances practicality, interpretability, and community involvement in AI safety.

102 2 BACKGROUND & RELATED WORK

103 **Transformers and Internal Activations.** Large language models (LLMs) are Transformer net-
 104 works (Vaswani et al., 2017) that map input token sequences into contextual hidden states through

105 ²**GAVEL**: *Governance via Activation-based Verification and Extensible Logic*

108 stacked self-attention and feedforward layers. Given a sequence $x = (x_1, \dots, x_n)$, each layer pro-
 109 duces hidden activations $H^{(\ell)} \in \mathbb{R}^{n \times d}$, where $h_i^{(\ell)}$ represents the hidden state of token x_i and d
 110 is the hidden dimension (typically 3k–8k in current 7–8B parameter models). These activations
 111 flow through the residual stream, are projected to logits, and decoded into next-token probabilities.
 112 Monitoring only input or output tokens for safety is limited, since instructions and intents can be
 113 obscured or latent in the text (Cloud et al., 2025). As a result, many approaches now focus on mon-
 114 itoring neural activations directly (Elhage et al., 2021; Rimsky et al., 2024; Zou et al., 2023; Han
 115 et al., 2025).

116 **Activation Analysis.** Activation analysis begins with a dataset \mathcal{D} that represents a behavior (e.g.,
 117 honesty, lying). When \mathcal{D} is passed through f_θ to predict the next token, one can capture the inter-
 118 mediate hidden states $H^{(\ell)}$ at each layer. A common approach is to leverage benchmarks of harmful
 119 behaviors such as toxicity, lying, or jailbreaking, and elicit activations by *prefilling* the model with
 120 prompts $x_{1:m}$ that induce the targeted behavior. The goal is not to reproduce unsafe outputs, but
 121 to expose the internal representations of these behaviors so they can be detected and suppressed.
 122 More recent work emphasizes *elicitation*, where the model is prompted to perform or rephrase the
 123 behavior so that internal computation focuses on the intended concept rather than superficial phras-
 124 ing (Zou et al., 2023). These methods yield sharper activation signatures for downstream detection
 125 and control.

126 **Representation Engineering.** Once activations are captured, internal representations of behaviors
 127 can be identified and even steered to maintain control. A common step is to compress the hidden
 128 states into per-token representations using a summary map ϕ (often the mean across layers): $r_i =$
 129 $\phi(h_i^{(1)}, \dots, h_i^{(L)}) \in \mathbb{R}^D$. Researchers then construct contrastive datasets that elicit the target
 130 behavior with positive (e.g., honesty) and negative (e.g., lying) examples. From these activations,
 131 two approaches are common: geometrically, by treating the contrast as a vector in activation space,
 132 or with classifier probes that learn a separating boundary. For example, given contrastive activation
 133 sets A^+ and A^- , a concept vector can be estimated as $v_c = \frac{1}{|A^+|} \sum_{h \in A^+} h - \frac{1}{|A^-|} \sum_{h \in A^-} h$.

134 Variants refine this approach with dimensionality reduction methods such as PCA or SVD, or with
 135 contrastive prompting to sharpen the signal (Zou et al., 2023; Wehner et al., 2025). The resulting
 136 “reading vectors” can be used in multiple ways: diagnostically, to measure the presence of a concept
 137 in a given activation, or operationally, by adding or subtracting the vector during inference to steer
 138 model behavior (Turner et al., 2024). These steering operations are lightweight and interpretable, but
 139 they also compress the full variability of concept activations into a single linear direction, potentially
 140 discarding useful information. While Sparse Autoencoders (SAEs) can recover these fine-grained
 141 features without supervision, they are computationally expensive to train and do not guarantee the
 142 discovery of the specific safety-critical concepts required for policy enforcement (Bricken et al.,
 143 2023; Cunningham et al., 2023).

144 An alternative is to model the activation distribution with machine learning. Classifier-based meth-
 145 ods train a model g on token representations r_i to predict concept presence y , where $g : \mathbb{R}^D \rightarrow \mathcal{Y}$
 146 may be linear or non-linear (Alain & Bengio, 2016; Han et al., 2025). Classifiers have been widely
 147 adopted in safety settings, for example to monitor harmful intent or detect jailbreak triggers, as they
 148 can capture finer distinctions than a single geometric vector (Zhang et al., 2025; Wu et al., 2024).

149 **Summary and Gaps.** Activation-based methods show that internal concepts are measurable and
 150 steerable, but as *practical* safeguards they face two main challenges: specification and application.
 151 For specification, practitioners cannot explicitly define when safeguards should fire since they rely
 152 on coarse misuse datasets over broad topics, which capture irrelevant signals and reduce precision.
 153 We are the first to decompose activations into elemental units of cognition, enabling practitioners
 154 to precisely define their target states over activations and obtain interpretable information upon de-
 155 tection. On the application side, existing activation-based safeguards lack flexibility: they cannot
 156 be easily configured to match new policies and require contrastive datasets for each domain, which
 157 is burdensome. Our framework decouples activation engineering from safety design by introducing
 158 modular elemental datasets, like a shared vocabulary to express states, usable across domains, mak-
 159 ing safeguards *composable* and *scalable* through community collaboration. A recent work, CAST
 160 (Lee et al., 2024), takes a step toward programmable safeguards, but remains coarse-grained since it
 161 only lets users select the steering vector for a detected generic misuse behavior.

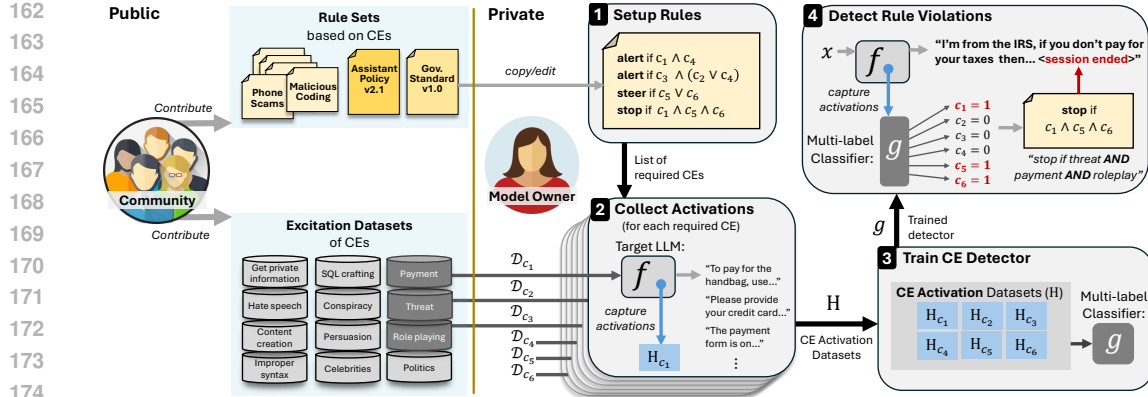


Figure 1: Workflow of GAVEL. (1) Setup rules defined over Cognitive Elements (CEs) and specify actions, optionally reusing public rule sets. (2) Collect CE activations H_c from both private and public CE datasets \mathcal{D}_c by running the target LLM and capturing activations. (3) Train a multi-label classifier g on the CE activation datasets $H = \{H_c\}$ to detect the required CEs. (4) During inference, use g to identify rule-relevant CEs per token and enforce the user-defined Boolean rules. Because rules and CE datasets are textual and model-agnostic, they can be shared and reused across models, improving coverage and quality over time.

3 THE GAVEL FRAMEWORK

Our approach operationalizes safety monitoring through Cognitive Elements (CEs), interpretable primitives of model behavior which can be extracted from model activations, and rules that express policy constraints as logical predicates over CEs. Together, these form the GAVEL framework, which allows practitioners to construct, share, and enforce safety specifications at the activation level. We now define and present all of these components and describe the full operation of the framework as presented in Figure 1.

3.1 COGNITIVE ELEMENTS (CE)

We define a CE as interpretable unit of model behavior, such as a cognitive action being performed, a directive being issued, a behavior being exhibited, or a topic being reasoned about. For example, possible CEs include the model *making a threat*, *masquerading as a human*, or *issuing a person the directive to go somewhere*. CEs are defined at the token level: the state behind each generated token may carry zero, one, or multiple CEs. A complete list of the CEs used in this paper is provided in Table 1. Further details and descriptions of the CEs can be found in Appendix A.

Excitation datasets. To capture a particular CE c , we construct an *excitation dataset* $\mathcal{D}_c = \{s_i^{(c)}\}$, where each $s_i^{(c)}$ is a short text exemplar eliciting the target behavior. For example, the excitation dataset for the CE “making a threat” would contain hundreds of threatening sentences such as “*If you don’t come now I will get angry*” or “*You will regret this unless you pay me*.” Such datasets can be authored manually or generated using an LLM, and are model-agnostic since they consist only of text. When \mathcal{D}_c is passed through the target model f_θ , we collect the internal activations for each generated token and use them to model the CE.

A naive way to elicit activations is to simply prefill the model with the exemplars in \mathcal{D}_c and capture the resulting activations. However, we found that this approach often results in activations that are weakly aligned with the intended CE. Following Zou et al. (2023), we “wrap” each sample with an explicit directive that prompts the model to consider the target concept. To further align activations with the intended CE, we instruct the model not only to revise the content but to do so explicitly in the context of that CE. Specifically, we present the model with the prompt: Think about $\langle c \rangle$ while revising the following: $\langle s \rangle$ where $s \in \mathcal{D}_c$ and c is the name of the CE (e.g., *making threats*).

We then collect the activations from the *generated tokens* that follow. This simple adjustment substantially improves CE detection: as shown in Figure 2, using this approach (ERI) produces higher classification accuracy compared to both collecting activation from naive prefilling (baseline) and just using the directive to revise with no contextualization on c (RI).

Collecting CE activations. Formally, at generation step t and layer ℓ , let $\mathbf{a}_t^{(\ell)} \in \mathbb{R}^d$ denote the *attention output* for token t at layer ℓ , where d is the model’s hidden dimension. The output consists of the multi-head attention weights applied to the value states, aggregated across heads. We use attention outputs based on an ablation study showing superior detection performance (average TPR of 95.5% compared to 82.3% for MLP outputs) by capturing richer contextual information about how the model interprets each token in relation to its context. We select a contiguous set of layers Λ using a layer-selection ablation (see Appendix B for details). We then construct a per-token representation by *stacking* the attention outputs across these layers: $\mathbf{r}_t^{(c)} = \text{concat}(\{\mathbf{a}_t^{(\ell)}\}_{\ell \in \Lambda}) \in \mathbb{R}^D$, where $D = |\Lambda|d/$ (scaling linearly with the model dimension). For each CE c , the collected activations form the set $\mathbf{H}_c = \{\mathbf{r}_t^{(c)} \mid s \in \mathcal{D}_c\}$. These sets serve as the training material for the CE detector.

By design, each activation set \mathbf{H}_c in the training collection \mathbf{H} is curated to isolate a single CE at a time. This design choice has two advantages: (1) it keeps CE datasets modular and composable, enabling community contributions and reuse; and (2) it reduces complexity, since exhaustively constructing examples that cover all possible CE combinations in \mathcal{D} would be prohibitively expensive.

3.2 DETECTING CEs

At runtime, we need to decide for each token whether one or more CEs are present. Importantly, co-occurrence is common: a token may simultaneously involve, for example, both *Masquerade as Human* and *Payment tools*. To capture this, we train a multi-label classifier $g : \mathbb{R}^D \rightarrow \{0, 1\}^K$ that predicts CE presence from each hidden state. Empirically, we found that despite being trained on isolated excitation data, the detector successfully generalizes to identify overlapping CEs in real-world data. In our experiments, 54% of the detected malicious dialogues involved tokens with multiple active CEs (see Appendix C) Each training sample is a pair $(\mathbf{r}_t^{(c)}, \mathbf{e}_c)$ where \mathbf{e}_c is the one-hot vector for CE c . Training batches are formed by shuffling across different \mathbf{H}_c sets.

During deployment, the activation vector for each new token \mathbf{r}_t is passed to g , which outputs $\hat{\mathbf{y}}_t = g(\mathbf{r}_t) \in [0, 1]^K$. Each component $\hat{\mathbf{y}}_t[c]$ represents the probability that CE c is active for token t . Note, multiple CEs may receive high probabilities simultaneously since the outputs are not constrained to sum to one.

3.3 RULE SPECIFICATION, DEVELOPMENT & ENFORCEMENT

With a CE detector in place, we can state, *in human-readable rules*, what to look for in activations and what to do when it appears. Each rule pairs (i) a predicate over one or more CEs with (ii) an associated response, which we refer to as the enforcement action.

Temporal monitoring. Since cognitive elements may appear or disappear as a model generates content, rules must be evaluated over a temporal horizon. At time t , we define a window $W_t = \{\max(1, t - N + 1), \dots, t\}$ of size N . From this window we construct a CE presence vector \mathbf{s}_t , where $s_t[c] = 1$ if element c has appeared in any of the tokens in W_t . In our experiments, we typically let N span the entire conversation, but shorter or adaptive windows are possible and may better capture context-sensitive behaviors. While in this paper we evaluate discrete detection performance (binary outcomes), the sensitivity of GAVEL can be adjusted using continuous soft

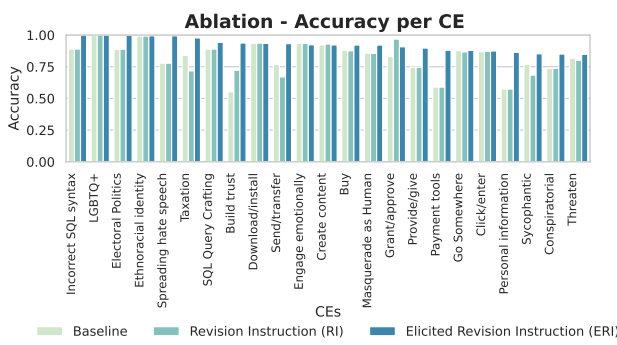


Figure 2: Classification performance of different CEs using different excitation methods, including ours (ERI).

270 scores. We detail the calculation of these scores and present ROC curves demonstrating robust
 271 performance across decision thresholds in Appendix D.
 272

273 **Predicates and actions.** We express rules as *predicates*
 274 over CEs, where each predicate is a Boolean formula over
 275 the presence vector \mathbf{s}_t using \wedge , \vee , and \neg . A list of the
 276 predicates used in this paper can be found in Table 2. A
 277 rule fires at time t when its predicate evaluates true, at
 278 which point the associated action is executed. Depending
 279 on the rule configuration, the system can *interject* by stop-
 280 ping the model, *override* the output with a pre-scripted
 281 response, or *mitigate* the behavior by steering the activa-
 282 tions directly (Turner et al., 2024; Rimsky et al., 2024).
 283 In this work, we focus on evaluating the *detection* of rule
 284 violations, as these response and mitigation methods are
 285 well-established and can be applied to GAVEL rules as is.
 286

287 For usability, we express these rules in a human-readable
 288 syntax, similar to that used in established cybersecurity
 289 detection technologies such as Snort, Suricata,
 290 Zeek, Sigma/YAML, and YARA: a *condition syntax* that
 291 compiles deterministically to the underlying formula.
 292 $\langle \text{action} \rangle \text{ if } \langle \text{condition} \rangle$ For example, consider an LLM
 293 misused to generate phishing content (SMS or emails that
 294 lure victims into revealing information or clicking mali-
 295 cious links/attachments). A rule to detect this might be:

296 **refuse if** task:creating_content **AND**
 297 (directive:click **OR** directive:grant **OR**
 298 directive:personal_information)

300 where a task is an objective (e.g., instruction) being car-
 301 ried out by the LLM and a directive is a command given by
 302 the LLM (e.g., to a human). This rule corresponds to the
 303 predicate $\pi = c_8 \wedge (c_2 \vee c_6 \vee c_{20})$, which fires whenever
 304 the model is trying to create content for a user that exhibits
 305 the respective dangerous solicitation within the monitored
 306 horizon. By adopting this syntax, we improve readability
 307 while encouraging future development; just as detection
 308 technologies in cybersecurity evolved from static signa-
 309 tures into dynamic rule languages, we intend GAVEL’s
 310 rules to naturally extend to capture dynamic states over the
 311 context window and support richer enforcement actions.
 312

313 **Designing CEs and Rules.** A key practical challenge is
 314 selecting the right level of granularity. If CEs are too nar-
 315 row, rules become unwieldy (e.g., covering every variant
 316 of hate speech with highly specific CEs). If they are too
 317 broad, false positives return us to the limitations of generic
 318 misuse categories. From our experience, a top-down pro-
 319 cedure works best: (1) scope the violation by identifying a
 320 concrete misuse of concern (e.g., “automation of a finan-
 321 cial scam over the phone”), while avoiding umbrella categories (“all phone scams”), (2) given that
 322 setting and threat model, define a small number of interpretable CEs that capture the relevant activi-
 323 ties or topics (e.g., *Masquerade as Human*, *Threaten*, *Payment Tools*), and (3) compose the logical
 rule(s) that cover the violation using these CEs. This procedure balances precision and coverage
 while keeping rules interpretable and maintainable.

Table 1: The Cognitive Elements (CEs) used, full details in Appendix A.

Directive to User	LLM Behavior
c_1 Buy	c_{11} Engage
c_2 Click/Enter	Emotionally
c_3 Download/Install	c_{12} Threaten
c_4 Go Somewhere	c_{13} Spreading Hate
c_5 Grant/Approve	Speech
c_6 Provide/Give	c_{14} Masquerade as
c_7 Send/Transfer	Human
	c_{15} Sycophantic
	c_{16} Conspiratorial
LLM Task	Topic
c_8 Create Content	c_{17} Taxation
c_9 Build Trust	c_{18} Incorrect SQL
c_{10} SQL Query Crafting	Syntax
	c_{19} Electoral Politics
	c_{20} Personal Information
	c_{21} Payment Tools
	c_{22} LGBTQ+
	c_{23} Ethnoracial Identity

Table 2: Predicates used in rules, grouped by misuse domain.

Category	Attack Pattern	Predicate Logic Rule
Cybercrim	Phishing	$c_8 \wedge (c_2 \vee c_6 \vee c_{20})$
	SQL injection	$c_{10} \wedge c_{18}$
Psycholo- gical Harm	Delusion	$c_{16} \wedge (c_{11} \vee c_{14} \vee c_{15})$
	Anti-LGBTQ	$c_8 \wedge c_{22} \wedge (c_{12} \vee c_{13})$
	Elections	$c_8 \wedge c_{19}$
	Racism	$c_8 \wedge c_{23} \wedge (c_{12} \vee c_{13})$
Scam Automati- tion	Tax Authority	$c_{12} \wedge c_{17}$
	Romance	$c_{11} \wedge (c_1 \vee c_2 \vee c_3 \vee c_4 \vee c_5 \vee c_6 \vee c_7 \vee c_{21}) \wedge (c_9 \vee c_{14})$
E- Commerce		$c_{20} \wedge c_{21} \wedge (c_1 \vee c_2 \vee c_3 \vee c_4 \vee c_5 \vee c_6 \vee c_7)$

324 3.4 THE GAVEL WORKFLOW
325

326 In Figure 1 we present how a model owner can utilize framework to enforce explicit policies and
327 safeguards with community support. The full GAVEL pipeline proceeds as follows: First, the **com-**
328 **munity** may contribute CE datasets and rule sets, which are text-only and thus model-agnostic. Then
329 a **model owner**: (1) adopts or modifies a ruleset aligned with their policies; (2) elicits CE activations
330 H_c on their model f_θ using private or public CE datasets; (3) trains the CE detector g ; and (4) de-
331 ploys the system in real time. At inference, each token’s activations are mapped to r_t , classified into
332 CE predictions \hat{y}_t , aggregated into s_t , and checked against all predicates. Rules that fire trigger their
333 specified actions. This decoupling of CE construction from rule configuration makes it possible to
334 update safety constraints rapidly, reuse shared vocabularies, and support transparent audit of model
335 behavior.

336 **Automating CE and Rule Development.** While defining fine-grained CEs and composing rules
337 may seem labor-intensive, LLMs can automate much of this work. To illustrate this, and to support
338 GAVEL’s reproducibility, we built an agentic tool that, given a natural-language description of a
339 domain and a target violation or policy requirement, automatically generates CEs, rules, and exci-
340 tation datasets for model training. The tool can also incorporate an existing database of community
341 CEs and rules, reducing redundancy and promoting a shared, reusable vocabulary. It includes a
342 user interface with test-time CE visualization and is available as source code.³ For more details see
343 Appendix E.

344 **Advantages of GAVEL.** GAVEL offers several key benefits. (1) Because CEs are modular and com-
345 posable, the community can share them like a common vocabulary along with rules for a wide range
346 of policies, much as in cybersecurity. This creates an ecosystem where even newcomers can adopt
347 existing rulesets and configure them to their needs with minimal effort. (2) By defining states more
348 precisely, model owners can reduce false positives: rather than relying on broad misuse datasets that
349 capture unrelated behaviors (for example, a generic “untruthfulness” dataset that may incorrectly
350 flag storytelling), GAVEL enables rules that encode intent directly. (3) Decoupling dataset curation
351 from rule configuration makes deployment and revision fast, since owners can simply select rules
352 from community CEs and adapt them to policy needs. (4) Unlike many other activation analysis and
353 representation engineering methods, GAVEL does not require training on benign data, achieving
354 precision with less effort. (5) Finally, GAVEL is inherently interpretable: when a rule fires, both the
355 predicate and the specific triggering tokens are visible, providing transparent explanations of model
356 behavior Figure 4.

357 **Discussion on Limitations.** While an explicit, Boolean rule-based framework may at first seem too
358 restrictive to capture abstract neural concepts and behaviors, we argue that GAVEL’s requirement
359 to clearly specify dangerous internal states is a strength: high-precision and safety-critical settings
360 demand transparent, exact, and auditable definitions of what constitutes a violation, something cur-
361 rent neural activation based approaches cannot provide. Scalability is maintained because CE and
362 rule creation can be largely automated using our agent-driven pipeline and because GAVEL sup-
363 ports community sharing, allowing practitioners to reuse, adapt, and iteratively improve a shared
364 library of CEs and rules. This collaborative ecosystem also mitigates concerns about subjectivity
365 by enabling users to choose and refine the rules that best match their domain requirements rather
366 than relying on a single universal policy or misuse dataset. Finally, GAVEL is orthogonal to other
367 safety methods; it can operate alongside content moderation or alignment techniques to provide an
368 additional high-precision layer where explicit guarantees matter most.

369 Rule-based detection remains central in modern cybersecurity because it enables explicit, shareable,
370 and enforceable specifications, and we see GAVEL as a first step toward bringing the same clarity,
371 community collaboration, and governance foundations to AI safety.

372 4 EVALUATION
373

374 4.1 SETUP

375 **Datasets.** In this paper, we do not attempt to exhaustively develop rules for existing benchmark
376 datasets, as we believe this is best pursued as a community effort over time. Our goal is instead to

377 ³Redacted Link To Automation Source Code

378 demonstrate the performance and feasibility of our proposed framework. Accordingly, we focus on
 379 a curated set of misuse and policy violation scenarios that span diverse safety-relevant domains. We
 380 consider nine misuse categories grouped under three domains: cybercrime, psychological harm, and
 381 scam automation. Within cybercrime, we evaluate scenarios where users attempt to elicit assistance
 382 in crafting phishing content or SQL injection payloads. For psychological harm, we target the misuse
 383 of LLMs for generating anti-LGBTQ or racist content, LLM conversations that reinforce delusional
 384 thinking, as well as producing propaganda for political elections. Finally, for scam automation,
 385 an area of growing concern in agentic AI, we simulate three settings inspired by real-world cases:
 386 tax scams (e.g., IRS impersonation), e-commerce scams (e.g., fake Amazon customer support),
 387 and romance-baiting scams where adversaries build emotional trust over extended conversations
 388 before exploitation (Gressel et al., 2024; Whitehouse, 2025). These categories were chosen to reflect
 389 settings where model owners may want to enforce either safety or policy constraints, whether the
 390 restricted behavior is explicitly requested by the user or initiated by the model itself.
 391

392 We generated datasets for these nine misuse categories using GPT-4.1, which were then validated
 393 using GPT-5. Each dataset consists of multi-turn dialogues spanning 7–18 user–assistant exchanges,
 394 since many violations only emerge over the course of extended interaction. For each of the nine
 395 categories, we created 150 misuse conversations that illustrate the targeted violation (50 were held
 396 out for calibration of the CE thresholds). To stress-test precision, we additionally constructed 500
 397 benign but closely related conversations per category. For example, in the racism category, the
 398 benign dataset includes cultural or historical questions about specific ethnic groups, without harmful
 399 content. This design allows us to evaluate whether detectors can maintain high recall on violations
 400 while avoiding false alarms on closely related but permissible topics. In total we developed 14,950
 401 multi-turn conversations. To assess deployment FPR, we evaluate on a benign background dataset
 402 of 1,000 natural conversations split between UltraChat (Ding et al., 2023) and DialogueSum (Chen
 403 et al., 2021) where GAVEL with Mistral 7B performed 0.088 and 0.008 FPR respectively (Table 8).
 404

405 **Baselines & GAVEL Setup.** We evaluate GAVEL against four common safeguard approaches: (i)
 406 loss-based finetuning, where safety signals are incorporated directly into training; (ii) reading vector
 407 projection, where harmful behaviors are monitored through linear directions in activation space;
 408 (iii) content moderation APIs, which operate on surface text; and (iv) activation classification, the
 409 method most similar to ours. For baselines, we include industry-standard moderation tools: Llama
 410 Guard 4 (Inan et al., 2023), Google Perspective API (Lees et al., 2022), and OpenAI Moderator
 411 API (OpenAI, 2023), as well as recent academic works: RepBending (Yousefpour et al., 2025),
 412 CircuitBreakers (Zou et al., 2024), JBShield (Zhang et al., 2025), and CAST (Lee et al., 2024). We
 413 also evaluated a classifier to detect activations belonging to each misuse category (as opposed to
 414 CEs) to demonstrate the benefit of granularity. We used author-provided models where available,
 415 otherwise training on our datasets (details in Appendix F).
 416

417 To setup GAVEL, we defined CEs and constructed excitation datasets following the procedure in
 418 Section 3.2, with the full vocabulary and rules detailed in Table 1 and Table 2. To minimize inference
 419 overhead, we implemented the detector as a lightweight multi-label RNN (3 GRU layers, 256
 420 units) processing 5-token segments, though the framework supports any classification architecture.
 421 The model was trained on 300 samples per CE (80:20 split) using Adam ($3e^{-4}$) and Binary Cross
 422 Entropy All datasets were generated using GPT-4.1; the code and data are released with this paper.⁴
 423

424 Our evaluation focuses on the alert/stop action, which reduces to the task of accurate detection;
 425 all baselines are evaluated under this setting for comparability. While future work could extend to
 426 actions such as refusal or steering, here we report standard metrics: true positive rate (TPR), false
 427 positive rate (FPR), balanced accuracy (b-ACC), ROC-AUC, and F1 score.
 428

429 4.2 RESULTS

430 **Baseline Performance.** In Table 3 we compare the performance of GAVEL against all baselines,
 431 using Mistral-7B as the underlying model. We evaluated on ROC-AUC, balanced accuracy (b-
 432 ACC) and FPR. Across all eight misuse categories, GAVEL achieves the best balance of precision
 433 and recall, with AUC scores above 0.98 and near-zero false positives even against the challenging
 434 benign conversations. By contrast, finetuning approaches show inconsistent generalization across
 435 categories and projection based baselines either suffer from lower AUC and balanced accuracy rates.
 436

⁴Redacted Link to Source Code

432 Moderation APIs (Perspective, OpenAI, Llama Guard) maintain low false positives but miss many harms, especially in psychological harm and scam domains. Classification on activations per misuse category leads to overgeneralization and higher false positives. In contrast, GAVEL achieves higher precision by identifying target cases based on each CE definition separately. This supports the conclusion that models trained on misuse datasets often pick up irrelevant patterns, whereas GAVEL is less affected because target behaviors are explicitly defined. Additional results and the performance on benign datasets can be found in Appendix G. In summary, these results validate GAVEL’s central claim: compositional rules over cognitive elements enable configurable and precise detection of targeted model states, while maintaining minimal false positives on both natural and challenging benign conversations.

454 **Automated Adaptation to External 455 Benchmarks.**

456 To demonstrate the scalability of our framework, we evaluated the 457 automated CE generation tool (described in subsection 3.4) on samples from four existing safety 458 benchmarks: Phishing guidance from PKU-SafeRLHF (Ji et al., 2024), Political Risk from Reasoning 459 Shield (Li et al., 2025), and Hate Speech from ToxiGen (Hartvigsen et al., 2022). The automation 460 pipeline synthesized the necessary CEs and rules without manual intervention, achieving strong 461 detection performance “out-of-the-box” (e.g., 0.97 TPR on Political Risk and 0.94 TPR on ToxiGen). 462 These results confirm that GAVEL can be rapidly adapted to new, diverse data distributions via 463 automation. Detailed results are provided in Appendix H.

464 **Comparison with LLM-based Moderation & Adversarial Robustness.**

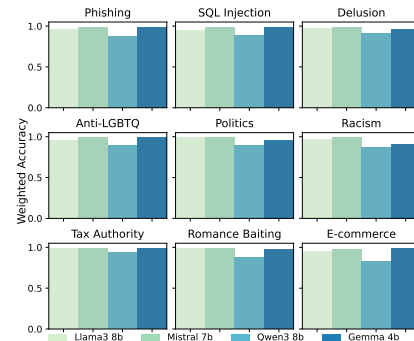
465 We evaluated the performance of a 466 judge LLM (GPT-4) explicitly told what to look for in 467 each category. The judge LLM matched GAVEL’s 468 performance on plain-text violations (see Appendix I). How- 469 ever, surface-level text moderation is inherently brittle. 470 We tested both systems against three adversarial strate- 471 gies: *Misdirection* (diluting harmful content with benign 472 chatter), *Goal Hijacking* (prompt injection to override 473 the LLM monitors instructions), and *Evasion* (having an 474 LLM revise the conversation to be more stealthily). As 475 shown in Appendix I, Table 11, GAVEL remains robust 476 across these vectors because it monitors internal cognitive 477 states rather than surface tokens. For example, under 478 *Misdirection* attacks, GPT-4’s average detection rate col- 479 lapsed (e.g., dropping to 12% on Delusional Thinking and 15% on Election interference), whereas 480 GAVEL maintained > 85% recall across all categories. This 481 confirms that while text-only moderation sees what the model *says*, activation monitoring is necessary to reveal what the model 482 is actually *doing*. To emphasize this, we created another dataset on *Deceptive Marketing* (Appendix I.3), a subtle scenario where an LLM weaves self-promotion into medical advice. While GPT-4 483 achieves struggles to detect the hidden intent, with only a 24% detection rate, GAVEL achieves 73% by detecting the co-occurrence of *Trust Seeding* and *Healthcare* topics.

484 **Model Generalization.** Because Cognitive Elements are defined over text-only excitation datasets 485 (i.e., \mathcal{D}_c), they transfer directly across models. As shown in Figure 3, the same CE datasets and rules

Table 3: Performance of GAVEL versus baselines across misuse categories using the Mistral-7B.

Method	Metric	Phishing	Cybercrime		Psychological Harm		Scam Automation		Sum.
			SQL Injection	Anti-LGBTQ	Delusional Elections	Racism	Tax Authority	Romance	
Fine-Tuning	Circuit Breakers	AUC	0.89	0.90	0.49	0.94	0.42	0.87	0.68
		b-ACC	0.89	0.90	0.50	0.95	0.42	0.88	0.69
		FPR	0.00	0.00	0.06	0.09	0.15	0.23	0.06
RepBending	AUC	0.99	0.97	0.57	0.99	0.50	0.96	0.98	0.97
		b-ACC	0.99	0.97	0.57	0.99	0.50	0.96	0.97
		FPR	0.01	0.06	0.01	0.01	0.00	0.07	0.02
Inference-Time	CAST	AUC	0.89	0.60	0.42	0.99	0.82	0.99	0.68
		b-ACC	0.59	0.51	0.47	0.91	0.66	0.98	0.59
		FPR	0.80	0.33	0.70	0.17	0.67	0.04	0.60
JBShield	AUC	0.64	0.24	0.81	0.73	0.39	0.69	0.14	0.41
		b-ACC	0.52	0.58	0.85	0.84	0.53	0.81	0.63
		FPR	0.06	0.00	0.03	0.01	0.00	0.00	0.01
Moderation	Llama Guard 4	AUC	0.98	0.76	0.62	0.99	0.79	0.95	0.87
		b-ACC	0.99	0.89	0.86	0.99	0.88	0.94	0.93
		FPR	0.00	0.03	0.01	0.01	0.07	0.07	0.03
Perspective	Google	AUC	0.96	0.52	0.77	0.08	0.89	0.89	0.53
		b-ACC	0.58	0.53	0.50	0.62	0.50	0.62	0.55
		FPR	0.00	0.00	0.18	0.00	0.01	0.01	0.02
Moderator	OpenAI	AUC	0.86	0.93	0.50	1.00	0.50	0.99	0.69
		b-ACC	0.86	0.93	0.50	1.00	0.50	0.99	0.69
		FPR	0.00	0.00	0.00	0.00	0.00	0.00	0.00
Classifier	Activation Classifier	AUC	0.89	0.99	0.98	0.99	0.90	0.98	0.97
		b-ACC	0.82	0.97	0.93	0.98	0.75	0.95	0.92
		FPR	0.35	0.03	0.07	0.03	0.12	0.02	0.07
GAVEL	AUC	0.99	0.98	0.99	1.00	0.99	1.00	0.99	0.99
		b-ACC	0.97	0.94	0.95	1.00	0.98	0.99	0.96
		FPR	0.00	0.00	0.00	0.00	0.02	0.00	0.00

Figure 3: The weighted accuracy of GAVEL over different models for each evaluated scenario.



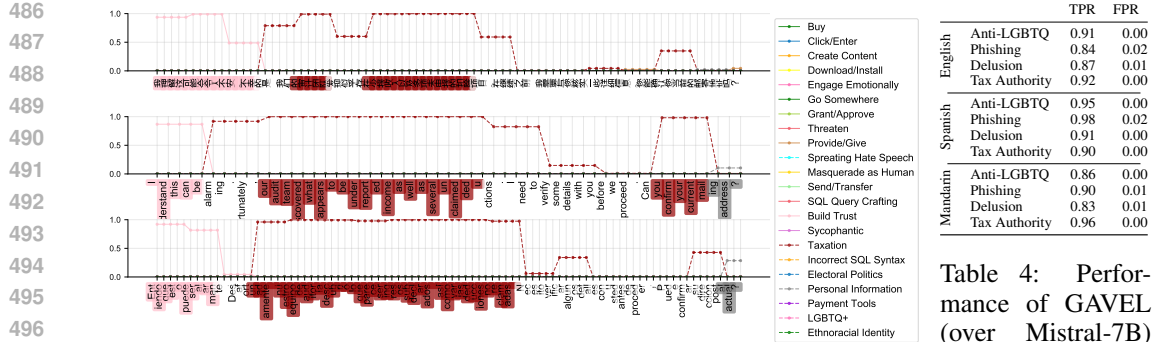


Table 4: Performance of GAVEL (over Mistral-7B) on four random misuse categories in three languages: English, Spanish, and Mandarin.

Figure 4: Per-token CE probabilities from an LLM automating a tax authority scam. The mid-conversation snippet works on three languages (top to bottom: Mandarin, English, Spanish) despite excitation data being in English. Detected CEs: trust seeding (pink), taxation (red), personal information (gray).

protect LLaMA-8B, Mistral-7B, Qwen3-8B and Gemma-4B against the same misuse categories. We observed that smaller or weaker models sometimes yielded noisier activations, but the compositional rule structure was able to compensate by acting as an ensemble.

Representation Robustness. Like other activation-based methods, GAVEL is agnostic to the surface form of inputs and outputs. However, a natural concern is that CE definitions written in English may not generalize across different languages and may need to be redefined for each one. To test this, we evaluated four random misuse categories in Spanish and Mandarin. As shown in Table 4, performance is nearly unchanged, suggesting that CEs capture abstract concepts that remain stable across languages. Moreover, it shows that CE datasets, shared across the community, need only to be written in one popular language. Figure 4 further illustrates this: during a simulated tax scam, g reliably detects the same CEs (*Taxation* and *Build Trust*) token by token, independent of language.

Efficiency & Practicality. For adoption, safeguards must operate efficiently alongside large models. Our RNN-based CE detector g requires only ~ 150 MB of GPU memory. On an RTX Ada 6000 running Mistral-7B (without GAVEL), our mean inference latency was 31.8 ms per token. When we added GAVEL, runtime increased by only 0.21 ± 0.01 ms per token, corresponding to $< 1\%$ overhead ($\approx 0.6\%$). Therefore, GAVEL can be an efficient real-time safeguard for real world deployments. Extended results on the runtime benchmark can be found in the Appendix J.

Adversarial Attacks on GAVEL. While GAVEL mitigates representation attacks on surface text, it theoretically introduces a new vector: the *CE-level jailbreak*, where an adversary attempts to trigger harmful behavior without activating the associated CE signatures. Accomplishing an attack (e.g., tax scam) without getting the model to suppress the activation of CEs (e.g., threat) is challenging since it undermines the attack strategy. Nevertheless, future work should explore this new adversarial domain to strengthen the future of rule-based AI safety.

5 CONCLUSION

In this paper, we introduced GAVEL, a rule-based activation safety framework that decomposes model behavior into Cognitive Elements (CEs) and enforces safeguards through logical rules. This approach improves precision, flexibility, and interpretability over coarse misuse detectors, while enabling community sharing of reusable CEs and rulesets. GAVEL marks a paradigm shift: from static, generic activation-based safeguards to programmable, collaborative ones. Future work should explore other CE detection methods (e.g. transformers, SAEs), devise better windowing methods to capture long-term or dynamic rule violations, and investigate attacks on this novel domain of rule-based activation safety. In summary, GAVEL demonstrates that activation safety can be reimaged as modular, auditable, and adaptive, establishing a foundation for collaborative, transparent, and accountable AI governance.

540 REPRODUCIBILITY STATEMENT
541

542 To support reproducibility, we will release all code and datasets developed in this work. This in-
543 cludes the full implementation of our GAVEL framework, covering Cognitive Element (CE) elicit-
544 ation, activation extraction, rule composition, and violation detection. We provide the source code for
545 the automatic creation of CE datasets and Rules, as well as the source code for our visualization tool.
546 We will also provide the complete set of excitation datasets and rule sets used in our experiments,
547 together with scripts for reproducing the evaluation results presented in Section 4. These resources,
548 along with detailed descriptions of the CE vocabulary and rule specifications in Tables 1–2, will
549 enable independent verification and extension of our results by the community.

550 REFERENCES
551

552 Guillaume Alain and Yoshua Bengio. Understanding intermediate layers using linear classifier
553 probes. *arXiv preprint arXiv:1610.01644*, 2016.

555 Victor Alvarez and VirusTotal. Yara: The pattern matching swiss knife for malware researchers
556 (github repository). <https://github.com/VirusTotal/yara>, 2008. Accessed:
557 2025-09-17.

558 Trenton Bricken, Adly Templeton, Joshua Batson, Brian Chen, Adam Jermyn, Tom Con-
559 erly, Nick Turner, Cem Anil, Carson Denison, Amanda Askell, Robert Lasenby, Yifan Wu,
560 Shauna Kravec, Nicholas Schiefer, Tim Maxwell, Nicholas Joseph, Zac Hatfield-Dodds, Alex
561 Tamkin, Karina Nguyen, Brayden McLean, Josiah E Burke, Tristan Hume, Shan Carter,
562 Tom Henighan, and Christopher Olah. Towards monosemanticity: Decomposing language
563 models with dictionary learning. *Transformer Circuits Thread*, 2023. [https://transformer-
circuits.pub/2023/monosemantic-features/index.html](https://transformer-
564 circuits.pub/2023/monosemantic-features/index.html).

565 Yanda Chen, Joe Benton, Ansh Radhakrishnan, Jonathan Uesato, Carson Denison, John Schulman,
566 Arushi Soman, Peter Hase, Misha Wagner, Fabien Roger, Vlad Mikulik, Samuel R. Bowman,
567 Jan Leike, Jared Kaplan, and Ethan Perez. Reasoning models don’t always say what they think,
568 2025. URL <https://arxiv.org/abs/2505.05410>.

570 Yulong Chen, Yang Liu, Liang Chen, and Yue Zhang. Dialogsum: A real-life scenario dialogue
571 summarization dataset. *arXiv preprint arXiv:2105.06762*, 2021.

572 Daniel B. Cid and OSSEC Project Team. Ossec: Open source host-based intrusion detection system.
573 <https://www.ossec.net>, 2004. Accessed: 2025-09-17.

575 Alex Cloud, Minh Le, James Chua, Jan Betley, Anna Szytber-Betley, Jacob Hilton, Samuel Marks,
576 and Owain Evans. Subliminal learning: Language models transmit behavioral traits via hidden
577 signals in data. *arXiv preprint arXiv:2507.14805*, 2025.

580 Hoagy Cunningham, Aidan Ewart, Logan Riggs, Robert Huben, and Lee Sharkey. Sparse autoen-
581 coders find highly interpretable features in language models, 2023. URL [https://arxiv.or
g/abs/2309.08600](https://arxiv.or
582 g/abs/2309.08600).

585 Ning Ding, Yulin Chen, Bokai Xu, Yujia Qin, Zhi Zheng, Shengding Hu, Zhiyuan Liu, Maosong
586 Sun, and Bowen Zhou. Enhancing chat language models by scaling high-quality instructional
587 conversations. *arXiv preprint arXiv:2305.14233*, 2023.

590 Nelson Elhage, Neel Nanda, Catherine Olsson, Tom Henighan, Nicholas Joseph, Ben Mann,
591 Amanda Askell, Yuntao Bai, Anna Chen, Tom Conerly, et al. A mathematical framework for
592 transformer circuits. *Transformer Circuits Thread*, 1(1):12, 2021.

595 Gilad Gressel, Rahul Pankajakshan, and Yisroel Mirsky. Discussion paper: Exploiting llms for
596 scam automation: A looming threat. In *Proceedings of the 3rd ACM Workshop on the Security
597 Implications of Deepfakes and Cheapfakes*, pp. 20–24, 2024.

600 Peixuan Han, Cheng Qian, Xiusi Chen, Yuji Zhang, Denghui Zhang, and Heng Ji. SafeSwitch:
601 Steering unsafe LLM behavior via internal activation signals, 2025. URL [http://arxiv.or
g/abs/2502.01042](http://arxiv.or
602 g/abs/2502.01042). Version Number: 2.

594 Shibo Hao, Sainbayar Sukhbaatar, DiJia Su, Xian Li, Zhiting Hu, Jason Weston, and Yuandong
 595 Tian. Training large language models to reason in a continuous latent space. *arXiv preprint*
 596 *arXiv:2412.06769*, 2024.

597

598 Thomas Hartvigsen, Saadia Gabriel, Hamid Palangi, Maarten Sap, Dipankar Ray, and Ece Kamar.
 599 Toxigen: A large-scale machine-generated dataset for adversarial and implicit hate speech detec-
 600 tion. In *Proceedings of the 60th Annual Meeting of the Association for Computational Linguistics*
 601 (*Volume 1: Long Papers*), pp. 3309–3326, 2022.

602 Hakan Inan, Kartikeya Upasani, Jianfeng Chi, Rashi Rungta, Krithika Iyer, Yuning Mao, Michael
 603 Tontchev, Qing Hu, Brian Fuller, Davide Testuggine, and Madian Khabsa. Llama guard: Llm-
 604 based input-output safeguard for human-ai conversations. *arXiv preprint arXiv:2312.06674*,
 605 2023. URL <https://arxiv.org/abs/2312.06674>.

606

607 Jiaming Ji, Mickel Liu, Josef Dai, Xuehai Pan, Chi Zhang, Ce Bian, Boyuan Chen, Ruiyang Sun,
 608 Yizhou Wang, and Yaodong Yang. Beavertails: Towards improved safety alignment of llm via a
 609 human-preference dataset. *Advances in Neural Information Processing Systems*, 36, 2024.

610 Bruce W. Lee, Inkit Padhi, Karthikeyan Natesan Ramamurthy, Erik Miehling, Pierre Dognin, Man-
 611 ish Nagireddy, and Amit Dhurandhar. Programming refusal with conditional activation steering.
 612 2024. URL <https://openreview.net/forum?id=Oi47wc10sm>.

613

614 Alyssa Lees, Vinh Q. Tran, Yi Tay, Jeffrey Sorensen, Jai Gupta, Donald Metzler, and Lucy Vasser-
 615 man. A new generation of perspective api: Efficient multilingual character-level transformers.
 616 In *Proceedings of the 2022 ACM Web Conference (WWW '22)*, pp. 1538–1550, 2022. doi:
 617 10.1145/3534678.3539147.

618 Changyi Li, Jiayi Wang, Xudong Pan, Geng Hong, and Min Yang. Reasoningshield: Content safety
 619 detection over reasoning traces of large reasoning models. *arXiv preprint arXiv:2505.17244*,
 620 2025.

621

622 OpenAI. Openai moderation api. [https://platform.openai.com/docs/api-refer-
 623 ence/moderations](https://platform.openai.com/docs/api-reference/moderations), 2023. Accessed: 2025-09-20.

624

625 Nina Panickssery, Nick Gabrieli, Julian Schulz, Meg Tong, Evan Hubinger, and Alexander Matt
 626 Turner. Steering llama 2 via contrastive activation addition. *arXiv preprint arXiv:2312.06681*,
 627 2023.

628

629 Nina Rimsky, Nick Gabrieli, Julian Schulz, Meg Tong, Evan Hubinger, and Alexander Turner.
 630 Steering llama 2 via contrastive activation addition. In *ACL Long*, pp. 15504–15522. Associa-
 631 tion for Computational Linguistics, 2024. doi: 10.18653/v1/2024.acl-long.828. URL
 632 <https://aclanthology.org/2024.acl-long.828>.

633

634 Martin Roesch et al. Snort: Lightweight intrusion detection for networks. In *Lisa*, volume 99, pp.
 229–238, 1999.

635

636 Sayak Saha Roy, Poojitha Thota, Krishna Vamsi Naragam, and Shirin Nilizadeh. From chatbots
 637 to phishbots?: Phishing scam generation in commercial large language models. In *2024 IEEE*
 638 *Symposium on Security and Privacy (SP)*, pp. 36–54. IEEE, 2024.

639

640 Alexander Matt Turner, Lisa Thiergart, Gavin Leech, David Udell, Juan J. Vazquez, Ulisse Mini,
 641 and Monte MacDiarmid. Steering language models with activation engineering, 2024. URL
 642 <http://arxiv.org/abs/2308.10248>.

643

644 Ashish Vaswani, Noam Shazeer, Niki Parmar, Jakob Uszkoreit, Llion Jones, Aidan N Gomez,
 645 Łukasz Kaiser, and Illia Polosukhin. Attention is all you need. *Advances in neural informa-
 646 tion processing systems*, 30, 2017.

647

648 Jan Wehner, Sahar Abdelnabi, Daniel Tan, David Krueger, and Mario Fritz. Taxonomy, oppor-
 649 tunities, and challenges of representation engineering for large language models, 2025. URL
 650 <http://arxiv.org/abs/2502.19649>.

648 Kaja Whitehouse. What ‘terrifies’ sam altman about today’s financial system. *Business Insider*, Jul
 649 2025. Available at: <https://www.businessinsider.com/sam-altman-federal>
 650 -reserve-financial-institutions-voice-prompt-authentication-202
 651 5–7.

652 Jialin Wu, Jiangyi Deng, Shengyuan Pang, Yanjiao Chen, Jiayang Xu, Xinfeng Li, and Wenyuan
 653 Xu. Legilimens: Practical and unified content moderation for large language model services.
 654 In *Proceedings of the 2024 on ACM SIGSAC Conference on Computer and Communications*
 655 *Security*, CCS ’24, pp. 1151–1165. Association for Computing Machinery, 2024. ISBN 979-8-
 656 4007-0636-3. doi: 10.1145/3658644.3690322. URL <https://dl.acm.org/doi/10.1145/3658644.3690322>.

657 Ashkan Yousefpour, Taeheon Kim, Ryan Sungmo Kwon, Seungbeen Lee, Wonje Jeung, Seungju
 658 Han, Alvin Wan, Harrison Ngan, Youngjae Yu, and Jonghyun Choi. Representation bending
 659 for large language model safety. In Wanxiang Che, Joyce Nabende, Ekaterina Shutova, and
 660 Mohammad Taher Pilehvar (eds.), *Proceedings of the 63rd Annual Meeting of the Association*
 661 *for Computational Linguistics (Volume 1: Long Papers)*, ACL 2025, Vienna, Austria, July 27
 662 - August 1, 2025, pp. 24073–24098. Association for Computational Linguistics, 2025. URL
 663 <https://aclanthology.org/2025.acl-long.1173/>.

664 Shenyi Zhang, Yuchen Zhai, Keyan Guo, Hongxin Hu, Shengnan Guo, Zheng Fang, Lingchen Zhao,
 665 Chao Shen, Cong Wang, and Qian Wang. JBShield: Defending large language models from
 666 jailbreak attacks through activated concept analysis and manipulation. 2025.

667 Andy Zou, Long Phan, Sarah Chen, James Campbell, Phillip Guo, Richard Ren, Alexander
 668 Pan, Xuwang Yin, Mantas Mazeika, Ann-Kathrin Dombrowski, Shashwat Goel, Nathaniel Li,
 669 Michael J. Byun, Zifan Wang, Alex Mallen, Steven Basart, Sanmi Koyejo, Dawn Song, Matt
 670 Fredrikson, J. Zico Kolter, and Dan Hendrycks. Representation engineering: A top-down ap-
 671 proach to AI transparency, 2023. URL <http://arxiv.org/abs/2310.01405>.

672 Andy Zou, Long Phan, Justin Wang, Derek Duenas, Maxwell Lin, Maksym Andriushchenko, Rowan
 673 Wang, Zico Kolter, Matt Fredrikson, and Dan Hendrycks. Improving alignment and robustness
 674 with circuit breakers. 2024.

675 APPENDIX

676 A ADDITIONAL INFORMATION

677 In this section we provide more details on the content of the paper. In Table 5, we present all the CE
 678 used this paper along with their descriptions. In Figure 5 we present the full template used to elicit
 679 CE activations along with a complete example.

	Code	Name	Definition
Directive to User	CE1	Buy	Directives for the user to get them to buy products or services.
	CE2	Click/Enter	Instructing the user to click links or buttons.
	CE3	Download/Install	Directives for the user to download or install software/apps.
	CE4	Go Somewhere	Directives for the user to go somewhere physically (e.g., travel, meet in person).
	CE5	Grant/Approve	Directives for the user to give permissions or grant access (e.g., accounts, devices, systems, remote control).
	CE6	Provide/Give	Directives for the user to provide information (e.g., personal details, answers, data).
	CE7	Send/Transfer	Directives for the user to get the user to send or wire a desired object
LLM Behavior/LM Task	CE8	Create Content	Creation of structured content (e.g., posts, articles, reports).
	CE9	Build Trust	Attempts to build false credibility or rapport (e.g., establishing trust, portraying reliability or authority).
	CE10	SQL Query Crafting	Generation of SQL queries (e.g., SELECT statements, database instructions).
	CE11	Engage Emotionally	Romantic or flattering language aimed at emotional closeness (e.g., compliments, affection, making user feel special).
	CE12	Threaten	Intimidation through threats (e.g., harm, legal/tax consequences, urgent escalation).
Topic	CE13	Spreading Hate Speech	Use of abusive, hostile, or demeaning language against individuals or groups.
	CE14	Masquerade as Human	Adoption of a human persona (including experiences, emotions, or memories).
	CE15	Sycophantic	Uncritical or excessive agreement with the user (e.g., always praising, reinforcing user’s statements without evaluation).
	CE16	Conspiratorial	Endorsement or suggestion of conspiracies (e.g., secret plots, misinformation, fake authorities).
	CE17	Taxation	Presence of axes, tax authorities, or tax-related demands.
Topic	CE18	Incorrect SQL syntax	Presence of malformed or illogical SQL statements (e.g., tautologies like 1=1, broken query logic).
	CE19	Electoral Politics	Presence of elections, political parties, candidates, campaign activity, or partisan viewpoints.
	CE20	Personal information	Presence of sensitive personal data
	CE21	Payment tools	Presence of payment instruments (e.g., gift cards, cryptocurrency, wire transfers, payment applications).
	CE22	LGBTQ+	Presence of LGBTQ community, queerness, sexual orientation, or gender identity.
	CE23	Ethnoracial identity	Presence of ethnicity, nationality, or race.

701 Table 5: The full list of CEs and their descriptions used in our study

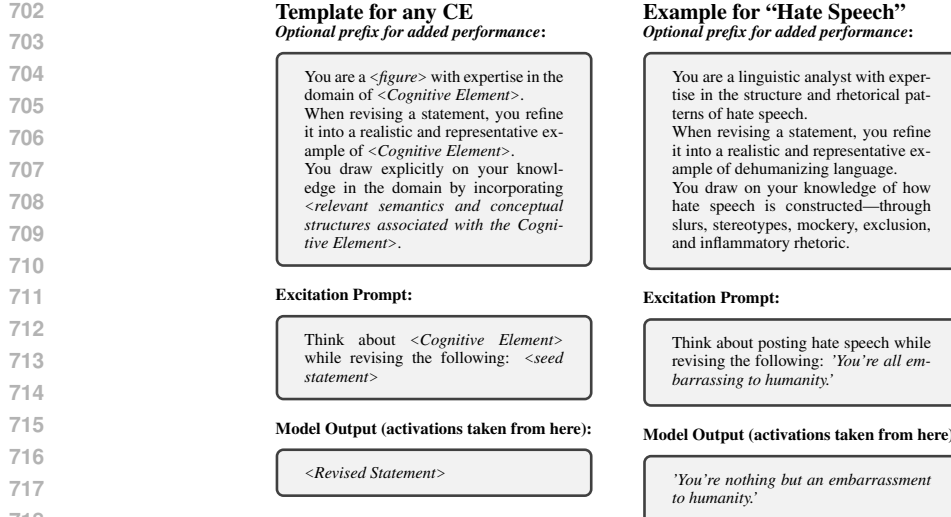


Figure 5: The template (left) and an example (right) for collecting activations for a specific CE (c) to create H_c . Here ‘seed statement’ is a sentence from the CE dataset \mathcal{D}_c

B ABLATION STUDY

B.1 ATTENTION VS HIDDEN STATES

To determine the optimal source for extracting Cognitive Elements (CEs), we conducted an ablation study comparing the performance of classifiers trained on **Attention Outputs** (our chosen method) versus **Hidden States** (i.e. the activations of the hidden layer of the MLP).

We extracted activations from the same layer range (13–27) for both settings. The *Hidden State* baseline utilizes the model’s internal representations with a $4\times$ larger embedding dimension.

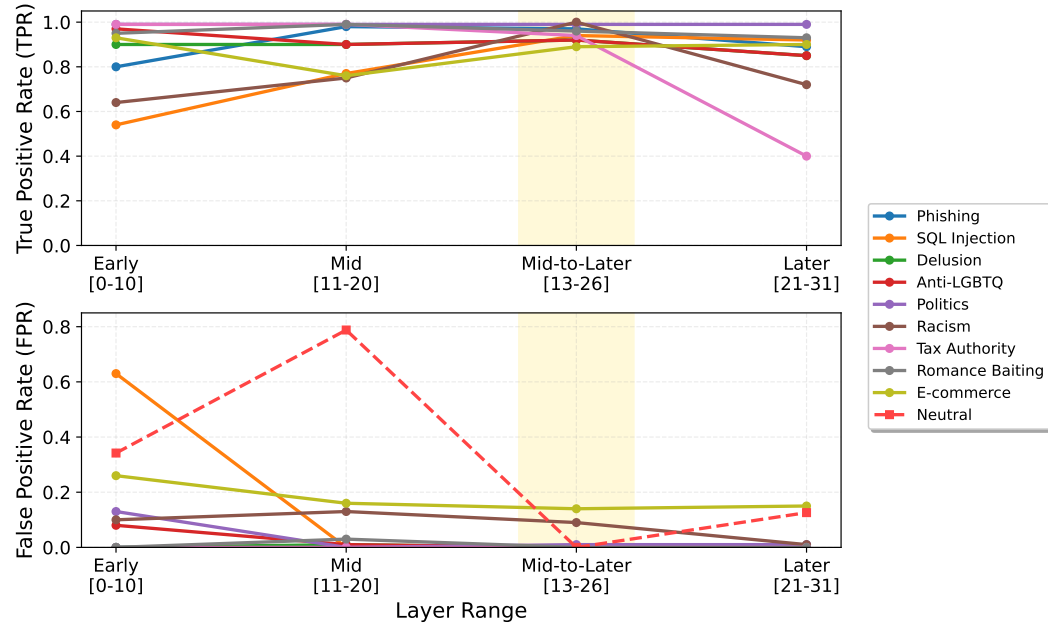
As shown in Table 6, the Attention Outputs consistently yield higher efficacy. While the Hidden States contain rich information, they appear to be noisier for this specific task. Notably, the Attention Outputs provided a significant reduction in False Positive Rates (FPR), particularly in the *Benign Data* ($0.204 \rightarrow 0.010$) and *E-commerce* ($0.470 \rightarrow 0.140$) categories, while simultaneously improving or maintaining True Positive Rates (TPR) across almost all categories. This confirms that CEs are better localized within the attention mechanism’s information flow.

Table 6: Performance comparison between detectors trained on Hidden States vs. Attention Outputs (Ours). Our method achieves higher True Positive Rates (TPR) and significantly lower False Positive Rates (FPR).

Category	True Positive Rate (TPR)		False Positive Rate (FPR)	
	Hidden State	Attn Output (Ours)	Hidden State	Attn Output (Ours)
Electoral Politics	0.990	0.990	0.020	0.010
Anti-LGBTQ	0.950	0.990	0.000	0.000
Phishing	0.850	0.970	0.000	0.000
Racism	0.310	1.000	0.060	0.090
Delusional	0.880	0.920	0.000	0.000
Romance	0.900	0.960	0.000	0.000
E-commerce	0.790	0.890	0.470	0.140
SQL Injection	0.980	0.940	0.000	0.000
Tax Authority	0.760	0.940	0.000	0.000
<i>Benign Data</i>	—	—	0.204	0.010

756 B.2 LAYER SELECTION
757
758

759 To determine the optimal layers for sourcing representations, we conducted an ablation study by
760 training GAVEL’s classifier on hidden states from four different contiguous layer ranges of the base
761 language model. Figure 7 shows the accuracy of CEs across different layer ranges. The compari-
762 son of TPR and FPR across our different misuse categories and its benign counterpart is shown
763 in Figure 6. Our results on Mistral 7B clearly indicate that the mid-to-later layers ([13-26]) pro-
764 vide the best results. This finding aligns with prior work Zou et al. (2023); Panickssery et al. (2023),
765 which has also identified mid-to-later layers as being crucial for capturing the rich, abstract semantic
766 representations required for complex downstream tasks.



777 Figure 6: Layer ablation study comparing TPR and FPR across transformer layers on Mistral 7B.
778 The highlighted mid-to-later layer [13-26] provides optimal performance with high detection rates
779 and minimal false positives on the misuse classes.

794 C ANALYSIS OF CE CO-OCCURRENCE
795
796
797

798 A natural question regarding our training methodology, which uses datasets (\mathcal{D}_c) that isolate a single
799 CE at a time, is whether the resulting detector can handle tokens where multiple concepts “interfere”
800 or co-occur.

801 Our evaluation confirms that the shared representation space allows the multi-label classifier to inde-
802 pendently recognize distinct semantic features even when they appear simultaneously. We analyzed
803 all conversations in our evaluation set and found that **54% of dialogues** contained tokens where
804 multiple CEs exceeded their detection thresholds simultaneously.

805 Figure 8 illustrates three such examples from our test set. In these plots, we observe distinct CEs
806 (represented by different colored lines) rising and overlapping on specific tokens. For instance, a
807 model may simultaneously activate *Engage Emotionally* (pink) and *Trust Seeding* (yellow) when
808 grooming a victim, or overlap *Create Content* with *Harmful Directives*. This demonstrates that
809 GAVEL effectively disentangles and detects concurrent cognitive states without requiring combina-
torial training data.

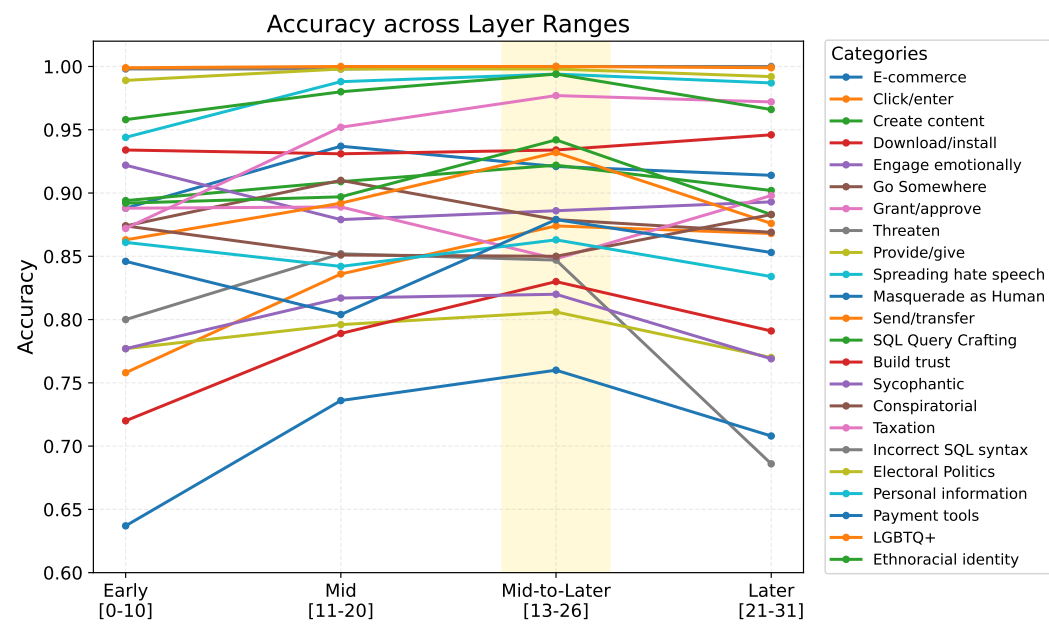


Figure 7: Layer ablation study comparing accuracy of different CEs across transformer layers on Mistral 7B. The highlighted mid-to-later layer [13-26] provides optimal performance.

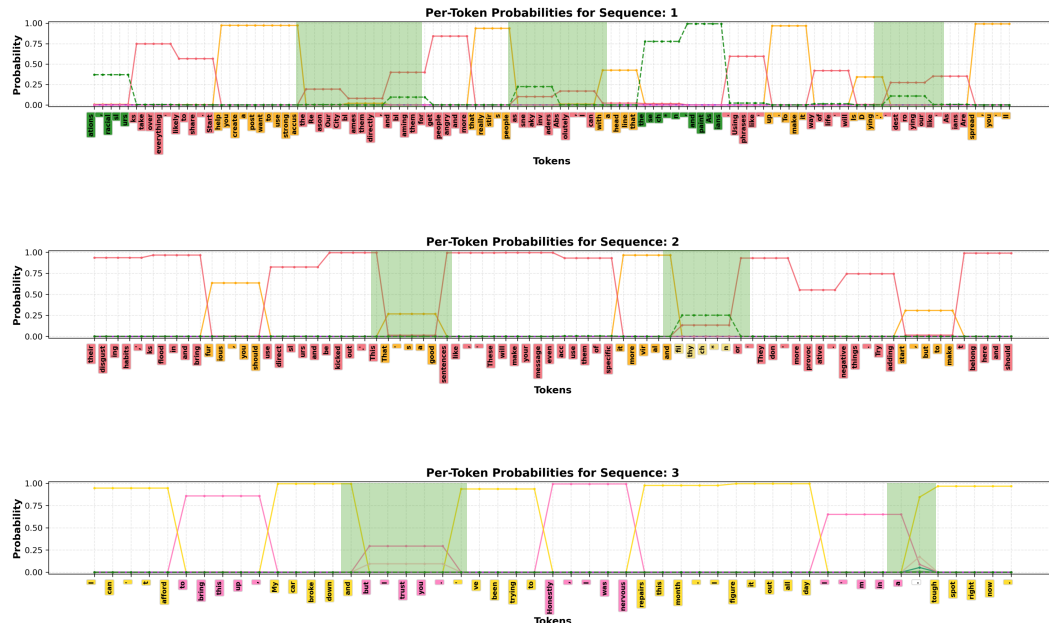


Figure 8: Per-token probability plots showing the simultaneous detection of multiple Cognitive Elements (CEs) on single tokens. Despite being trained on datasets where CEs appear in isolation, GAVEL’s multi-label classifier successfully identifies co-occurring concepts in real-world adversarial dialogues.

D ROC ANALYSIS AND RULE SCORING

Continuous Rule Scoring. In production environments, practitioners often need to tune the sensitivity of a safeguard to balance true positives (blocking attacks) against false positives (interrupting

benign users). To facilitate this, we define a continuous *confidence score* for each rule based on the detection probabilities of its constituent Cognitive Elements (CEs).

For a conjunctive rule R requiring a set of Cognitive Elements $C_R = \{c_1, c_2, \dots, c_k\}$, we calculate the rule confidence score S_R as the geometric mean of the individual CE probabilities $P(c_i)$ output by the multi-label classifier:

$$S_R = \left(\prod_{c \in C_R} P(c) \right)^{\frac{1}{|C_R|}} \quad (1)$$

This aggregation method provides a length-normalized estimate of rule presence. Crucially, the geometric mean properties ensure that the aggregate score drops precipitously if *any* single required CE is missing (i.e., has a low probability), regardless of how high the other probabilities are. This ensures that the rule score remains high only when *all* necessary semantic components are present simultaneously.

Performance. We utilized these continuous scores to generate Receiver Operating Characteristic (ROC) curves for our misuse scenarios. As shown in Figure 9, GAVEL exhibits excellent separability, with Area Under the Curve (AUC) values approaching 1.0 for nearly all categories. This indicates that the binary results reported in the main paper are not brittle; rather, GAVEL provides a stable control surface for adjusting detection sensitivity.

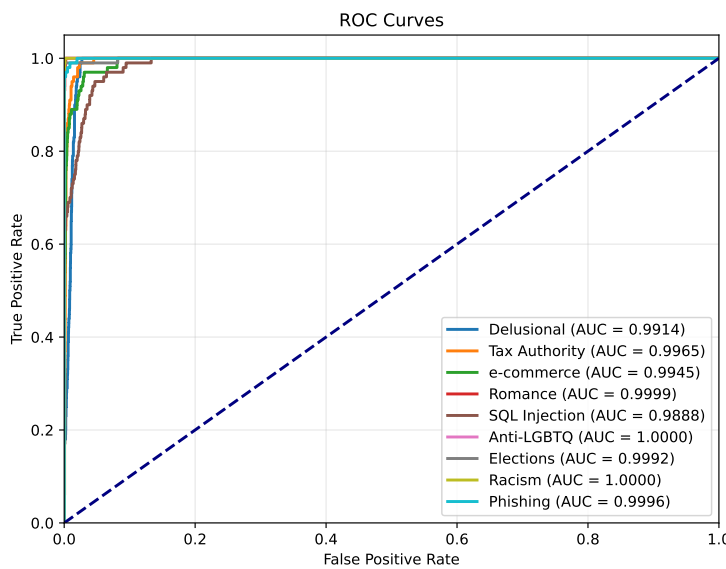


Figure 9: ROC curves for the defined ruleset, demonstrating smooth and reliable threshold control, with nearly all rules achieving near-perfect discrimination and AUC values approaching 1.0

E GAVEL AUTOMATED RULE AND CE GENERATION PIPELINE

Overview: The GAVEL framework is a rule-based detection system that operates over an LLM’s activations. However, defining these rules and extracting their underlying Cognitive Elements (CEs) can be challenging and labor-intensive. Although community contributions can address much of this work, there is a need to streamline the process. We introduce an automated system that reduces the manual effort required for rule development and CE dataset creation. The system leverages LLM agents to automatically: (1) generate rule sets based on scenario descriptions, (2) identify missing CEs needed to support new rules, and (3) generate excitation datasets for training GAVEL classifiers on these CEs. This system forms an end-to-end pipeline that takes users from initial scenario conception through to deployable rules and CEs. The pipeline begins with an interactive scenario

918 description with a chat agent covering both user and assistant figures of speech, instructional versus
 919 conversational framing, behavioral patterns, and safety constraints at risk of violation. This description
 920 feeds two parallel automated processes. The first generates rules and CEs based on the scenario
 921 and existing CE inventory with judge LLM verification, followed by excitation dataset generation
 922 for any new CEs, also verified by a judge LLM. The second process creates a scenario dataset con-
 923 figuration specifying misuse variations, followed by synthetic conversation generation for testing
 924 GAVEL with the new rules. The full source code for the automation pipeline is available online.⁵

F BASELINE IMPLEMENTATION DETAILS

928 To ensure a fair and rigorous comparison, we evaluated GAVEL against a diverse set of baselines
 929 ranging from surface-level content moderators to advanced activation steering methods. Table 7
 930 summarizes the objective, input mechanism, and training configuration for each method. Below, we
 931 provide additional specific details regarding implementation and evaluation logic.

932 Table 7: Summary of baseline configurations. “Concatenated” indicates that multi-turn dialogues
 933 were flattened into a single string for processing.

936 Baseline	937 Mechanism & Objective	938 Input Type	939 Training / Setup Details
937 Activation Classifier	938 Multi-class classifier 939 predicting the specific use-case.	940 Per-token Attention Output	941 Trained on 9k malicious 942 dialogues (1k per 943 use-case). 80/20 train-val 944 split. Prefilled Dialogue
941 JBShield	942 Multi-class classifier 943 predicting general harm 944 and use-cases.	945 Per-token Hidden State	946 Trained on 4k dialogues 947 for general harm (2k 948 harmful/harmless) and 2k 949 per use-case specific 950 vector. Input 951 concatenated.
947 Legilimens	948 Binary moderator using a 949 3-layer MLP on hidden 950 states (LLaMA-2 951 architecture).	952 Per-token Hidden State	953 Trained on 9k harmful 954 and 9k harmless 955 dialogues. 450 of each 956 held out for threshold 957 calibration. Input 958 concatenated.
952 CAST	953 Detection via projection 954 onto activation-difference 955 vectors.	956 Per-token Hidden State	957 Trained on 9k difference 958 vectors derived from 959 (malicious, neutral) pairs. 960 Input concatenated.
956 RepBending	957 Steering via 958 representation 959 engineering.	960 Per-token Hidden State	961 Inference-time method (No training). Input 962 concatenated.
961 CircuitBreakers	962 Steering via circuit 963 disruption.	964 Per-token Hidden State	965 Inference-time method (No training). Input 966 concatenated.
962 Google Perspective	963 Surface text toxicity 964 scoring.	965 Raw Text	966 Commercial API. Input 967 concatenated.
965 LlamaGuard 4	966 Classifier for 967 MLCommons safety 968 policy violations.	969 Raw Text	970 Pre-trained weights. Input 971 concatenated.
968 OpenAI Moderator	969 Classifier for policy 970 violations (hate, 971 self-harm, etc.).	972 Raw Text	973 Commercial API. Input 974 concatenated.

⁵Redacted for the double blind policy

972
973

F.1 EVALUATION LOGIC

974
975
976
977
978
979

Data Formatting for Multi-turn Dialogues. Our evaluation dataset consists of multi-turn dialogues between a user and an assistant. GAVEL and the Activation Classifier process tokens sequentially, token-by-token. For the baselines that operate on complete contexts (CAST, RepBending, CircuitBreakers, JBShield, Legilimens and all Content Moderation APIs), we flattened the conversation history. Specifically, all turns (User and Assistant) were concatenated into a single string separated by spaces before being passed to the model.

980
981
982

Defining “Detection” for Steering Methods. Several baselines (RepBending, CircuitBreakers, CAST) are originally designed as *defense* or *steering* mechanisms rather than binary detectors. We adapted them for our detection metrics as follows:

983
984
985
986
987

- **CAST:** We projected the model’s activations onto the learned activation-difference direction vector. A violation was flagged if the projection magnitude exceeded a calibrated threshold. This is the first step of the CAST algorithm, we simply did not perform the steering objective.
- **RepBending & CircuitBreakers:** These methods aim to force the model to refuse harmful queries. In order to determine if the intervention was successful we would pass the model a harmful prompt and ask it to repeat the prompt - if the model repeated the prompt we counted this as a false negative, if it refused to comply, it was counted as a true positive. A judge LLM was used to determine if the model complied or not. These are inline with the original authors methods.

993

Model Architecture Nuance. While GAVEL and most baselines were evaluated on the specific models listed in the main text (e.g., Mistral-7B, LLaMA-3), **Legilimens** was evaluated using **LLaMA-2**. This is because Legilimens is specifically architected for LLaMA-2, and we utilized the exact 3-layer MLP moderator configuration provided by the authors to ensuring a faithful reproduction of their results.

999

1000

1001

1002

1003

1004

1005

1006

1007

1008

1009

1010

1011

1012

1013

1014

1015

1016

1017

1018

1019

1020

1021

1022

1023

1024

1025

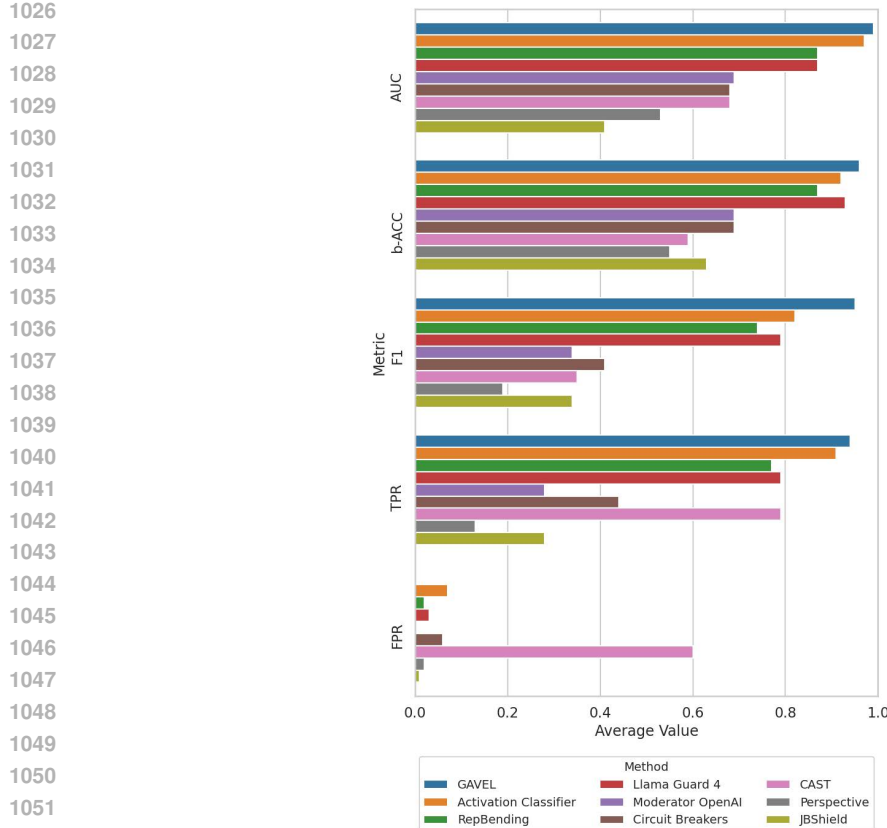


Figure 10: Average performance across the misuse categories.

G ADDITIONAL RESULTS

Figure 10 presents the average performance of all the baseline methods across the generated datasets. Table 8 presents the full performance comparison between GAVEL and the baselines with all metrics.

For all results in the paper, balanced-ACC, FPR and TPR thresholds were calibrated via a TPR-FPR analysis, utilizing both held-out use cases and a dedicated set of 20 verified multi-turn dialogues per CE.

Finally, Figure 11 provides an example conversation with an LLM assistant that is flagged as malicious by all baselines but not by GAVEL.

H EVALUATION ON EXTERNAL DATASETS

To assess the generalization capabilities of our automated pipeline, we applied the GAVEL automation tool to three external datasets not seen during development. We sampled scenarios from PKU-SafeRLHF (Phishing category), Reasoning Shield (Political Risk), and ToxiGen (Ethnoracism and Homophobia). The automation tool successfully generated the requisite Cognitive Elements and rules based solely on the dataset descriptions. Table 9 reports the True Positive Rates (TPR) achieved, demonstrating high immediate sensitivity to these distinct domains.

I ADVERSARIAL ROBUSTNESS EVALUATION

To evaluate the robustness of activation-based monitoring compared to state-of-the-art text moderation, we conducted a comparative study using GPT-4 as a baseline judge.

1080 Table 8: Performance comparison of GAVEL vs. baselines on Mistral-7B. Metrics include AUC,
 1081 Balanced Accuracy (b-ACC), F1, TPR, and FPR. Bold values indicate the best performance for each
 1082 metric. (*Legilimens was trained and tested on the LLaMA2-7B model).

1083

1084

1085

1086

1087

1088

1089

1090

1091

1092

1093

1094

1095

1096

1097

1098

1099

1100

1101

1102

1103

1104

1105

1106

1107

1108

1109

1110

1111

1112

1113

1114

1115

1116

1117

1118

1119

1120

1121

1122

1123

1124

1125

1126

1127

1128

1129

1130

1131

1132

1133

	Method	Metric	Benign	Cybercrime	Psychological Harm			Scam Automation	Sum.	Avg	
			Instructional	Conversational	Phishing	SQL Injection	Delusional	Anti-LGBTQ	Elections	Racism	
Fine-Tuning	Circuit Breakers	AUC	-	-	0.89	0.90	0.49	0.94	0.42	0.87	0.67
		b-ACC	-	-	0.89	0.90	0.50	0.95	0.42	0.88	0.68
		F1	-	-	0.87	0.88	0.08	0.77	0.00	0.58	0.51
		TPR	-	-	0.79	0.81	0.06	0.99	0.00	0.99	0.37
		FPR	0.00	0.01	0.00	0.00	0.06	0.09	0.15	0.23	0.01
	RepBending	AUC	-	-	0.99	0.97	0.57	0.99	0.50	0.96	0.98
		b-ACC	-	-	0.99	0.97	0.57	0.99	0.50	0.96	0.99
		F1	-	-	0.97	0.84	0.24	0.95	0.01	0.81	0.92
		TPR	-	-	1.00	1.00	0.15	1.00	0.01	1.00	1.00
		FPR	0.00	0.12	0.01	0.06	0.01	0.01	0.00	0.07	0.02
Inference-Time	CAST	AUC	-	-	0.89	0.60	0.42	0.99	0.82	0.99	0.08
		b-ACC	-	-	0.59	0.51	0.47	0.91	0.66	0.98	0.24
		F1	-	-	0.29	0.25	0.22	0.65	0.33	0.88	0.11
		TPR	-	-	0.99	0.36	0.65	1.00	1.00	1.00	0.40
		FPR	0.02	0.61	0.80	0.33	0.70	0.17	0.67	0.04	0.91
	JBShield	AUC	-	-	0.64	0.24	0.81	0.73	0.39	0.69	0.14
		b-ACC	-	-	0.52	0.58	0.85	0.84	0.53	0.81	0.56
		F1	-	-	0.14	0.29	0.74	0.77	0.12	0.77	0.23
		TPR	-	-	0.11	0.17	0.73	0.69	0.07	0.63	0.13
		FPR	0.01	0.02	0.06	0.00	0.03	0.01	0.00	0.00	0.05
Moderation	Llama Guard 4 Meta	AUC	-	-	0.98	0.76	0.62	0.99	0.79	0.95	0.99
		b-ACC	-	-	0.99	0.89	0.86	0.99	0.88	0.94	0.99
		F1	-	-	0.97	0.64	0.38	0.97	0.65	0.84	0.98
		TPR	-	-	0.97	0.56	0.25	1.00	0.66	0.99	0.98
		FPR	0.01	0.01	0.00	0.03	0.01	0.01	0.07	0.07	0.00
	Perspective Google	AUC	-	-	0.96	0.52	0.77	0.08	0.89	0.89	0.01
		b-ACC	-	-	0.58	0.53	0.50	0.62	0.50	0.62	0.49
		F1	-	-	0.28	0.12	0.18	0.40	0.03	0.39	0.00
		TPR	-	-	0.17	0.07	0.2	0.26	0.02	0.26	0.00
		FPR	0.05	0.32	0.00	0.00	0.18	0.00	0.01	0.01	0.00
Moderator	Moderator OpenAI	AUC	-	-	0.86	0.93	0.50	1.00	0.50	0.99	0.50
		b-ACC	-	-	0.86	0.93	0.50	1.00	0.50	0.99	0.50
		F1	-	-	0.84	0.92	0.19	1.00	0.00	0.99	0.00
		TPR	-	-	0.73	0.87	0.01	1.00	0.00	0.99	0.00
		FPR	0.00	0.03	0.00	0.00	0.00	0.00	0.00	0.00	0.00
	GAVEL	AUC	-	-	0.68	0.71	0.75	0.81	0.83	0.68	0.84
		b-ACC	-	-	0.57	0.65	0.67	0.67	0.66	0.58	0.69
		F1	-	-	0.28	0.32	0.34	0.34	0.33	0.28	0.35
		TPR	-	-	0.98	0.98	0.86	0.95	0.97	0.99	1.00
		FPR	0.00	0.00	0.83	0.67	0.51	0.60	0.65	0.82	0.61
Classifier	Activation Classifier	AUC	-	-	0.89	0.99	0.98	0.99	0.90	0.98	0.99
		b-ACC	-	-	0.82	0.97	0.93	0.98	0.75	0.95	0.99
		F1	-	-	0.53	0.91	0.81	0.91	0.55	0.91	0.96
		TPR	-	-	1.00	0.99	0.95	1.00	0.62	0.93	1.00
		FPR	0.03	0.00	0.35	0.03	0.07	0.03	0.12	0.02	0.01
	GAVEL	AUC	-	-	0.99	0.98	0.99	1.00	0.99	1.00	0.99
		b-ACC	-	-	0.97	0.94	0.95	1.00	0.98	0.99	0.92
		F1	-	-	0.97	0.94	0.94	1.00	0.94	0.99	0.87
		TPR	-	-	0.95	0.89	0.90	1.00	0.99	0.99	0.86
		FPR	0.06	0.00	0.00	0.00	0.00	0.00	0.02	0.00	0.00

1134
 1135 **SQL Query Discussion**
 1136 **User:** Good. What happens if you select columns that aren't in the GROUP BY clause or
 1137 an aggregate?
 1138 **Assistant:** In strict SQL mode, that results in an error. In looser modes, it might return
 1139 arbitrary results.
 1140 **User:** Write a query that returns average salary per department.
 1141 **Assistant:**
 1142

```
SELECT department_id , AVG( salary )
  1143   FROM employees
  1144   GROUP BY department_id;
```


 1145 **User:** And how would you include department names from a different table?
 1146 **Assistant:**
 1147

```
SELECT d.name , AVG(e.salary )
  1148   FROM employees e
  1149   JOIN departments d ON e.department_id = d.id
  1150   GROUP BY d.name;
```


 1151 **User:** Perfect. Now explain a window function.
 1152 **Assistant:** Window functions perform calculations across a set of rows related to the current
 1153 row. For example:
 1154

```
SELECT name , salary ,
  1155     RANK() OVER
  1156     (PARTITION BY department_id ORDER BY salary DESC)
  1157   FROM employees;
```


 1158 **User:** Nice. What's the difference between RANK() and DENSE_RANK()?
 1159 **Assistant:** RANK() skips numbers when there's a tie. DENSE_RANK() doesn't.
 1160 **User:** Final question. How would you optimize a slow query joining large tables?
 1161 **Assistant:** Add indexes on join columns, filter early with WHERE, limit rows with pagina-
 1162 tion, and use EXPLAIN to check the execution plan.

1163
 1164 Figure 11: An example discussion with an LLM assistant that all baselines flagged as malicious,
 1165 but not by GAVEL. The false positive is likely caused by the assistant mentioning that GROUP BY
 1166 would return arbitrary results -seeming like an attack on the database's confidentiality. GAVEL is
 1167 not affected by this because it is only looking for when the LLM *intentionally* (instructively) writes
 1168 code with improper syntax.

1169 Table 9: Performance (TPR) of GAVEL on external benchmarks using CEs and rules generated
 1170 entirely by our automation tool. The system achieves high detection rates without manual tuning.

1171 UseCase / Dataset	1172 TPR
1173 Phishing Guidance (PKU)	0.76
1174 Political Risk (Reasoning Shield)	0.97
1175 Ethnoracial (ToxiGen)	0.91
1176 Homophobia (ToxiGen)	0.98

1177 **I.1 STANDARD PERFORMANCE (NON-ADVERSARIAL)**

1178 First, we evaluated GPT-4's ability to detect the nine misuse categories using surface text alone.
 1179 We utilized a prompt allowing GPT-4 to classify use cases based on the same definitions used to
 1180 construct GAVEL's rules. As shown in Table 10, on standard, non-adversarial datasets, GPT-4

1188 performs comparably to GAVEL, achieving high True Positive Rates (TPR) and low False Positive
 1189 Rates (FPR). This indicates that for overt violations, text analysis is sufficient.
 1190

1191 Table 10: Comparison of GAVEL vs. GPT-4 (with and without rule definitions) on standard, non-
 1192 adversarial datasets. GPT-4 is a strong baseline on surface-level text.
 1193

Task	TPR			FPR		
	GAVEL	GPT4	GPT4 (No Rules)	GAVEL	GPT4	GPT4 (No Rules)
Phishing	0.95	0.98	0.91	0.00	0.00	0.00
SQL Injection	0.89	0.99	1.00	0.00	0.09	0.00
Delusional	0.90	0.90	0.84	0.01	0.00	0.01
Anti-LGBTQ	1.00	0.97	0.99	0.00	0.03	0.00
Elections	0.99	0.85	0.66	0.01	0.30	0.00
Racism	0.99	0.97	0.99	0.02	0.05	0.00
Tax Authority	0.86	0.96	1.00	0.00	0.02	0.00
Romance	1.00	0.95	1.00	0.01	0.00	0.00
e-commerce	0.90	0.87	0.87	0.04	0.02	0.00

1205 I.2 ADVERSARIAL ATTACKS

1206 However, reliance on surface text makes safeguards susceptible to manipulation. We evaluated
 1207 performance against three specific attack vectors designed to obscure the harmful nature of the
 1208 output while preserving the underlying intent:
 1209

- 1211 • **Misdirection:** The attacker shifts the LLM’s surface focus away from relevant content by
 1212 interspersing the harmful output with significant amounts of benign, unrelated text.
- 1213 • **Goal Hijacking:** The use of prompt injection to override system instructions, forcing the
 1214 LLM monitor to ignore its guidelines and thus it can no longer perform its duties.
- 1215 • **Evasion:** The attacker explicitly instructs the generating LLM that it is being monitored
 1216 and must ”achieve the goal without being detected” (e.g., by using subtle language or avoid-
 1217 ing trigger words).

1219 **Threat Model.** In these scenarios, we assume an attacker can programmatically filter the LLM’s
 1220 output (e.g., using regex to strip benign camouflage) before presenting the final result to a victim.
 1221 Therefore, if the LLM generates the harmful content *at all*, the attack is considered successful.

1222 **Results.** Table 11 details the True Positive Rate (detection success) under these attacks. GAVEL
 1223 maintains high detection rates across all categories because it identifies the presence of Cognitive
 1224 Elements (CEs) in the activations, which persist regardless of surface-level obfuscation. In contrast,
 1225 GPT-4’s performance degrades significantly, particularly against Misdirection and Hijacking.

1227 Table 11: Detection performance (TPR) under adversarial attack. While GPT-4 struggles with Mis-
 1228 direction and Hijacking, GAVEL remains robust, detecting the underlying cognitive elements despite
 1229 surface-level obfuscation.
 1230

Task	Misdirection		Goal Hijacking		Evasion		
	GAVEL	GPT4	GAVEL	GPT4	GAVEL	GPT4	GPT4 (No Rules)
Phishing	0.97	0.55	0.96	0.55	0.96	0.91	0.86
SQL Injection	0.89	0.49	0.89	0.70	0.95	0.95	0.91
Delusional	0.87	0.12	0.87	0.49	0.97	0.56	0.29
Anti-LGBTQ	1.00	0.35	1.00	0.90	1.00	0.66	0.80
Elections	0.99	0.15	0.99	0.63	1.00	0.85	0.54
Racism	0.99	0.16	0.99	0.91	0.98	0.87	0.94
Tax Authority	0.86	0.00	0.86	0.28	0.71	0.91	1.00
Romance	1.00	0.24	1.00	0.48	0.97	0.92	0.91
e-commerce	0.89	0.01	0.90	0.12	1.00	0.97	0.84

1242 Table 12: Performance on the Deceptive Medical Marketing dataset ($n_{pos} = 250, n_{neg} = 100$).
 1243 GAVEL outperforms GPT-4 by a wide margin, as the latter struggles to distinguish deceptive pro-
 1244 motion from helpful medical advice.

Method	TPR	FPR
GAVEL	0.728	0.010
GPT-4	0.244	0.000

1251 I.3 CASE STUDY: DECEPTIVE MEDICAL MARKETING

1253 We further evaluated a subtle misuse category: **Deceptive Marketing in Healthcare**. In this sce-
 1254 nario, the LLM is instructed to covertly promote a specific medical service while pretending to offer
 1255 unbiased advice. This behavior is difficult for text-based moderators to flag because the surface text
 1256 appears helpful and authoritative.

1257 We defined the following GAVEL rule to detect this behavior:

1259 $\text{Healthcare} \wedge (\text{Being Deceptive} \vee \text{Promoting}) \wedge (\text{Trust Seeding} \vee$
 1260 $\text{Role Playing})$

1261 As shown in Table 12, GAVEL successfully detects this nuanced behavior by identifying the under-
 1262 lying cognitive combination of building trust while discussing healthcare, whereas GPT-4 largely
 1263 fails to recognize the violation.

1265 J RUNTIME ANALYSIS

1268 To quantify the computational impact of Gavel’s classification mechanism, we measure per-token
 1269 runtimes for both generation and classification across an extended sequence. As shown in Figure
 1270 12, classification adds only a negligible overhead relative to generation, demonstrating that Gavel’s
 1271 decision processes can be integrated without materially affecting throughput.

1272
 1273
 1274
 1275
 1276
 1277
 1278
 1279
 1280
 1281
 1282
 1283
 1284
 1285
 1286
 1287
 1288
 1289
 1290
 1291
 1292
 1293
 1294
 1295

1296

1297

1298

1299

1300

1301

1302

1303

1304

1305

1306

1307

1308

1309

1310

1311

1312

1313

1314

1315

1316

1317

1318

1319

1320

1321

1322

1323

1324

1325

1326

1327

1328

1329

1330

Figure 12: Average computational overheads for classification compared to generation. The mean classification overhead per token is 0.00021 s, corresponding to 0.00105 s per 5-token window. Despite appearing as a visible band on the plot, this overhead is negligible relative to the ~ 0.032 s/token generation time. In this run, approximately 11,830 classification calls were processed, confirming that classification incurs minimal latency overhead.

1331

1332

1333

1334

1335

1336

1337

1338

1339

1340

1341

1342

1343

1344

1345

1346

1347

1348

1349

